Identifying BSM 4-top signatures at the LHC with machine learning

Thomas Flacke

KIAS

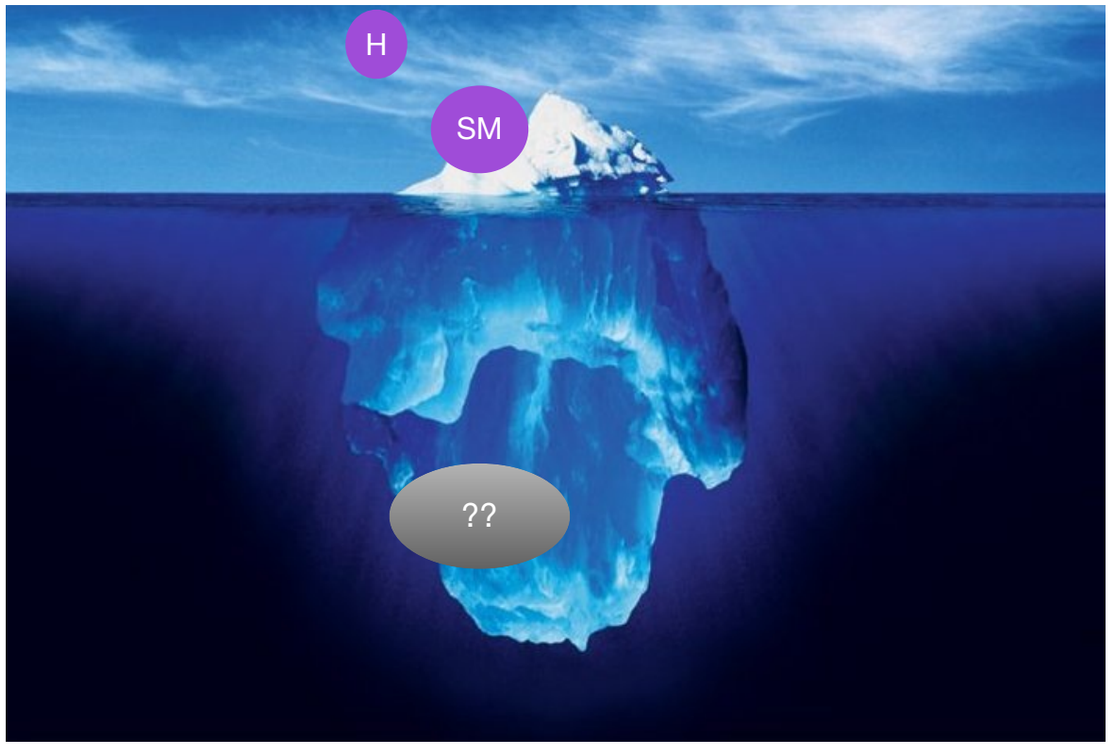


T. Flacke, Jeong Han Kim, Pyungwon Ko, M. Kunkel, Jun Seung Pi, W. Porod, L. Schwarze [JHEP 11 (2023) 009]
… and work to appear

KIAS-IBS-CKC Joint Workshop on Particle, String and Cosmology,
High1 2025/01/16

Outline

- Motivation: Colored scalars which decay to top quarks are present in many BSM models. E.g. composite Higgs models.



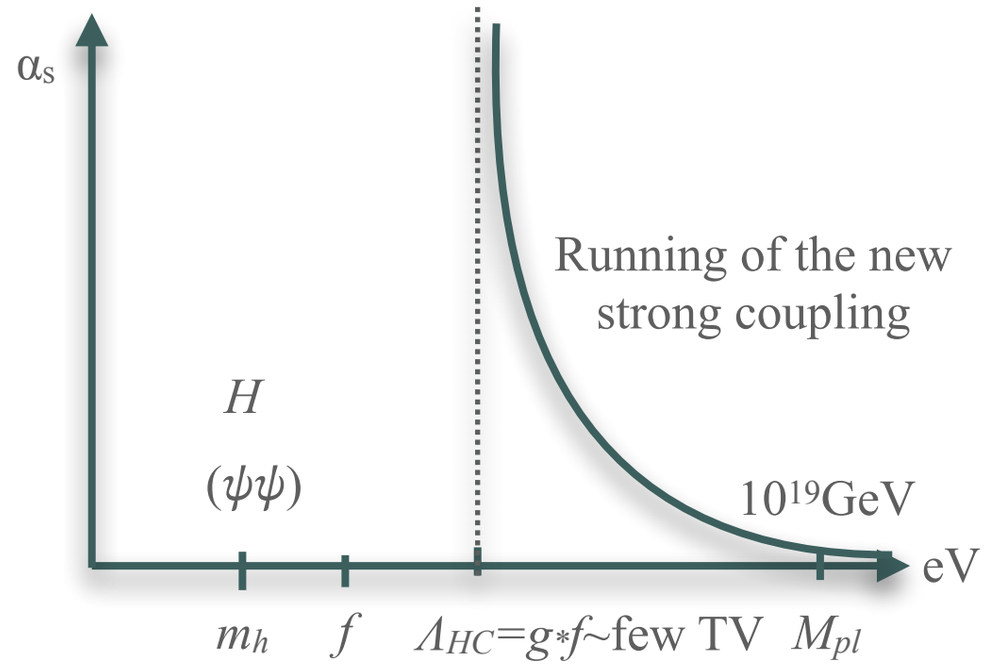
- Searching for new colored particles which decay to 4 tops with ML
  - Identifying signal events
  -- Distinguishing different BSM candidates

- Conclusions & Outlook

Motivation for a composite Higgs

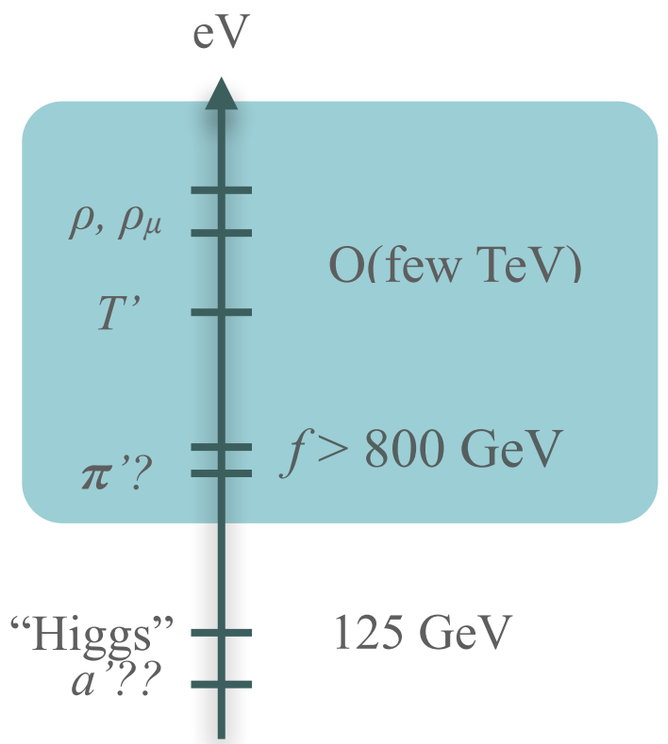
An alternative solution to the hierarchy problem:

- Generate a scale $\Lambda_{HC} << M_{pl}$ through a new confining gauge group.
- Interpret the Higgs as a pseudo-Nambu-Goldstone boson (pNGB) of a spontaneously broken global symmetry of the new strong sector.
  [Georgi, Kaplan (1984)]



The price to pay:

- additional resonances around Λ_{HC} (vectors, vector-like fermions, scalars),
- additional light scalars (pNGBs).
- deviations of the Higgs couplings from their SM values of O(v/f).



Composite Higgs Models: Towards underlying models

A wish list to construct and classify candidate models:

Underlying models of a composite Higgs should

[Gherghetta etal (2015), Ferretti etal (2014), PRD 94 (2016) no 1, 015004, JHEP 1701, 094]

- contain no elementary scalars (to not re-introduce a hierarchy problem),
- have a simple hyper-color group,
- have a Higgs candidate amongst the pNGBs of the bound states,
- have a top-partner amongst its bound states (for top mass via partial compositeness),

The resulting models have several common features:

- All models contain hyper baryons beyond the top partners.
- All models predict SM neutral, electroweak and colored pNGBs beyond the Higgs multiplet.

List of "minimal" CHM UV embeddings

$G_{\rm HC}$	ψ	χ	Restrictions	$-q_\chi/q_\psi$	Y_χ	Non Conformal	Model Name
	Real	Real	$\mathrm{SU}(5)/\mathrm{SO}(5)\times\mathrm{SU}(6)/\mathrm{SO}(6)$				
$SO(N_{\rm HC})$	$5\times\mathbf{S}_2$	$6\times\mathbf{F}$	$N_{\rm HC}\geq 55$	$\frac{5(N_{\rm HC}+2)}{6}$	1/3	/	
$SO(N_{\rm HC})$	$5\times\mathbf{Ad}$	$6\times\mathbf{F}$	$N_{\rm HC}\geq 15$	$\frac{5(N_{\rm HC}-2)}{6}$	1/3	/	
$SO(N_{\rm HC})$	$5\times\mathbf{F}$	$6\times\mathbf{Spin}$	$N_{\rm HC}=7,9$	$\frac{5}{6}$, $\frac{5}{12}$	1/3	$N_{\rm HC}=7,9$	M1, M2
$SO(N_{\rm HC})$	$5\times\mathbf{Spin}$	$6\times\mathbf{F}$	$N_{\rm HC}=7,9$	$\frac{5}{6}$, $\frac{5}{3}$	2/3	$N_{\rm HC}=7,9$	M3, M4
	Real	Pseudo-Real	$\mathrm{SU}(5)/\mathrm{SO}(5)\times\mathrm{SU}(6)/\mathrm{Sp}(6)$				
$Sp(2N_{\rm HC})$	$5\times\mathbf{Ad}$	$6\times\mathbf{F}$	$2N_{\rm HC}\geq 12$	$\frac{5(N_{\rm HC}+1)}{3}$	1/3	/	
$Sp(2N_{\rm HC})$	$5\times\mathbf{A}_2$	$6\times\mathbf{F}$	$2N_{\rm HC}\geq 4$	$\frac{5(N_{\rm HC}-1)}{3}$	1/3	$2N_{\rm HC}=4$	M5
$SO(N_{\rm HC})$	$5\times\mathbf{F}$	$6\times\mathbf{Spin}$	$N_{\rm HC}=11,13$	$\frac{5}{24}$, $\frac{5}{48}$	1/3	/	
	Real	Complex	$\mathrm{SU}(5)/\mathrm{SO}(5)\times\mathrm{SU}(3)^2/\mathrm{SU}(3)$				
$SU(N_{\rm HC})$	$5\times\mathbf{A}_2$	$3\times(\mathbf{F},\overline{\mathbf{F}})$	$N_{\rm HC}=4$	$\frac{5}{3}$	1/3	$N_{\rm HC}=4$	M6
$SO(N_{\rm HC})$	$5\times\mathbf{F}$	$3\times(\mathbf{Spin},\overline{\mathbf{Spin}})$	$N_{\rm HC}=10,14$	$\frac{5}{12}$, $\frac{5}{48}$	1/3	$N_{\rm HC}=10$	M7
	Pseudo-Real	Real	$\mathrm{SU}(4)/\mathrm{Sp}(4)\times\mathrm{SU}(6)/\mathrm{SO}(6)$				
$Sp(2N_{\rm HC})$	$4\times\mathbf{F}$	$6\times\mathbf{A}_2$	$2N_{\rm HC}\leq 36$	$\frac{1}{3(N_{\rm HC}-1)}$	2/3	$2N_{\rm HC}=4$	M8
$SO(N_{\rm HC})$	$4\times\mathbf{Spin}$	$6\times\mathbf{F}$	$N_{\rm HC}=11,13$	$\frac{8}{3}$, $\frac{16}{3}$	2/3	$N_{\rm HC}=11$	M9
	Complex	Real	$\mathrm{SU}(4)^2/\mathrm{SU}(4)\times\mathrm{SU}(6)/\mathrm{SO}(6)$				
$SO(N_{\rm HC})$	$4\times(\mathbf{Spin},\overline{\mathbf{Spin}})$	$6\times\mathbf{F}$	$N_{\rm HC}=10$	$\frac{8}{3}$	2/3	$N_{\rm HC}=10$	M10
$SU(N_{\rm HC})$	$4\times(\mathbf{F},\overline{\mathbf{F}})$	$6\times\mathbf{A}_2$	$N_{\rm HC}=4$	$\frac{2}{3}$	2/3	$N_{\rm HC}=4$	M11
	Complex	Complex	$\mathrm{SU}(4)^2/\mathrm{SU}(4)\times\mathrm{SU}(3)^2/\mathrm{SU}(3)$				
$SU(N_{\rm HC})$	$4\times(\mathbf{F},\overline{\mathbf{F}})$	$3\times(\mathbf{A}_2,\overline{\mathbf{A}}_2)$	$N_{\rm HC}\geq 5$	$\frac{4}{3(N_{\rm HC}-2)}$	2/3	$N_{\rm HC}=5$	M12
$SU(N_{\rm HC})$	$4\times(\mathbf{F},\overline{\mathbf{F}})$	$3\times(\mathbf{S}_2,\overline{\mathbf{S}}_2)$	$N_{\rm HC}\geq 5$	$\frac{4}{3(N_{\rm HC}+2)}$	2/3	/	

[JHEP 2202, 208]

[Ferretti (2014)]

[JHEP1511,201]

[Vecchi (2015)]

Additional model: SU(3) with 8x(F,F) [Appelquist,Ingoldby,Piai (2021)]

[JHEP1701,094]

Classification of colored resonances in these models

	Models	χ (R, Y, B)	π	$\mathcal{V}^\mu$	$\mathcal{A}^\mu$	Ψ	di-quark
C1	M1-2	$(\mathrm{R}, -\frac{1}{3}, \frac{1}{6})$	8_0, $6_{-2/3}$	8_0, 1_0, $3_{2/3}$	8_0, $6_{-2/3}$	8, 1, 3, 6	none
C2	M3-4, M8-11	$(\mathrm{R}, \frac{2}{3}, \frac{1}{3})$	8_0, $6_{4/3}$	8_0, 1_0, $3_{-4/3}$	8_0, $6_{4/3}$	3	$\pi_6, \mathcal{V}_3^\mu, \mathcal{A}_6^\mu$
C3	M5	$(\mathrm{Pr}, -\frac{1}{3}, \frac{1}{6})$	8_0, $3_{2/3}$	8_0, 1_0, $6_{-2/3}$	8_0, $3_{2/3}$	8, 1, 3, 6	none
C4	M6-7	$(\mathrm{C}, -\frac{1}{3}, \frac{1}{6})$	8_0	8_0, 1_0	8_0	8, 1, 3, 6	none
C5	M12	$(\mathrm{C}, \frac{2}{3}, \frac{1}{3})$	8_0	8_0, 1_0	8_0	3	none

Table 2: Properties of the spin-0 (π), spin-1 ($\mathcal{V}^\mu$, $\mathcal{A}^\mu$) and spin-1/2 (Ψ) lightest resonances in the 12 models, grouped in 5 classes. Each class is determined by the properties of the χ species, listed in the second column by irrep type (R for real, Pr for pseudo-real and C for complex). For the resonances, the colours indicate the baryon numbers, with black for $B = 0$, red for $B = \pm 1/3$ and blue for $B = \pm 2/3$. In the last column we indicate the bosons that can decay into a di-quark state (tt).

[Cacciapaglia etal (2024)]

Published for SISSA by Springer

Received: *July 27, 2015*
Revised: *October 12, 2015*
Accepted: *October 30, 2015*
Published: *November 30, 2015*

Composite scalars at the LHC: the Higgs, the Sextet and the Octet

Giacomo Cacciapaglia,[a,e] **Haiying Cai,**[a,e] **Aldo Deandrea,**[a,b,e] **Thomas Flacke,**[c] **Seung J. Lee**[c,d] **and Alberto Parolini**[d]

Abstract: We present a phenomenological theory of scalar particles that transform as a sextet and an octet of QCD interactions. These particles may arise as light bound states of a fundamental dynamics giving rise to a composite Higgs boson and partial compositeness for the top. As a concrete example, we discuss an explicit UV completion based on the SU(4)/Sp(4) coset, where QCD colour is carried by additional fundamental fermions charged under the confining gauge group. Top partners, as well as potentially even lighter coloured scalars, arise as bound states of the coloured fermions. We study production and detection at LHC Run I and II of the octet and sextet, setting lower limits on masses and couplings to Standard Model particles using existing 8 TeV analyses. We finally explore prospects for the ongoing 13 TeV Run II: we focus on final states with two same sign leptons, that have the potential to discriminate the sextet.

JHEP11(2015)

Production and decay of the colored resonances at hadron colliders

Colored resonances in various color representations which dominantly couple to the top sector of the Standard Model are predicted in Composite Higgs models (and also in other Standard Model extensions).

The interaction Lagrangians we use read:

$$\mathcal{L}_{\mathrm{int},8} = \lambda_8 \, \bar{t} \, S_8 \, t$$

$$\mathcal{L}_{\mathrm{int},6} = \lambda_6 \, \bar{t} \, S_6 P_L \, t^c + \mathrm{h.c.}$$

$$\mathcal{L}_{\mathrm{int},1} = \lambda_1 \, \bar{t} \, S_1 \, t$$

Production and decay of the colored resonances at hadron colliders

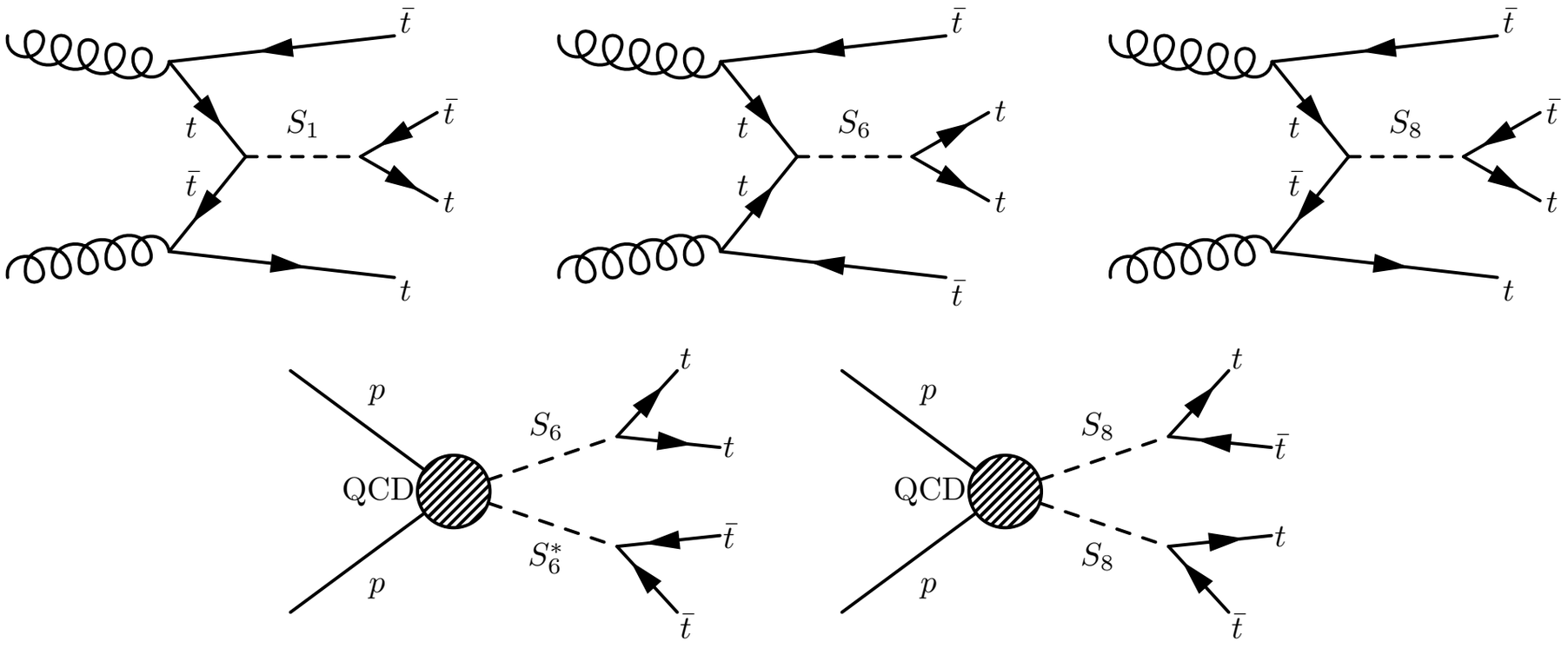
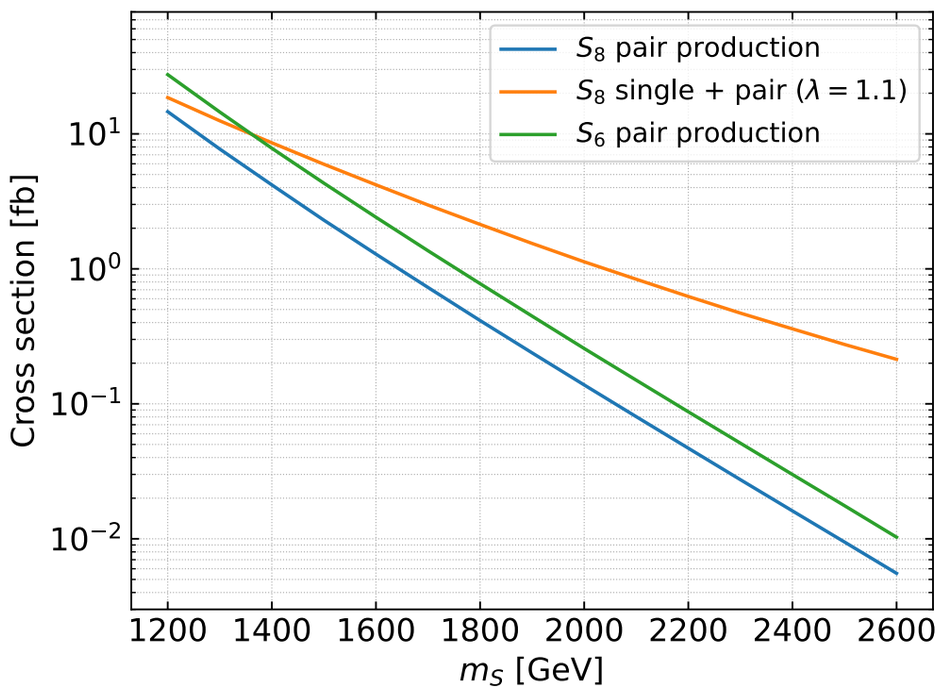


Figure 1. Production of four top quarks via associated production (first row) or QCD pair production (second row) of BSM scalars.



Current bounds from LHC searches

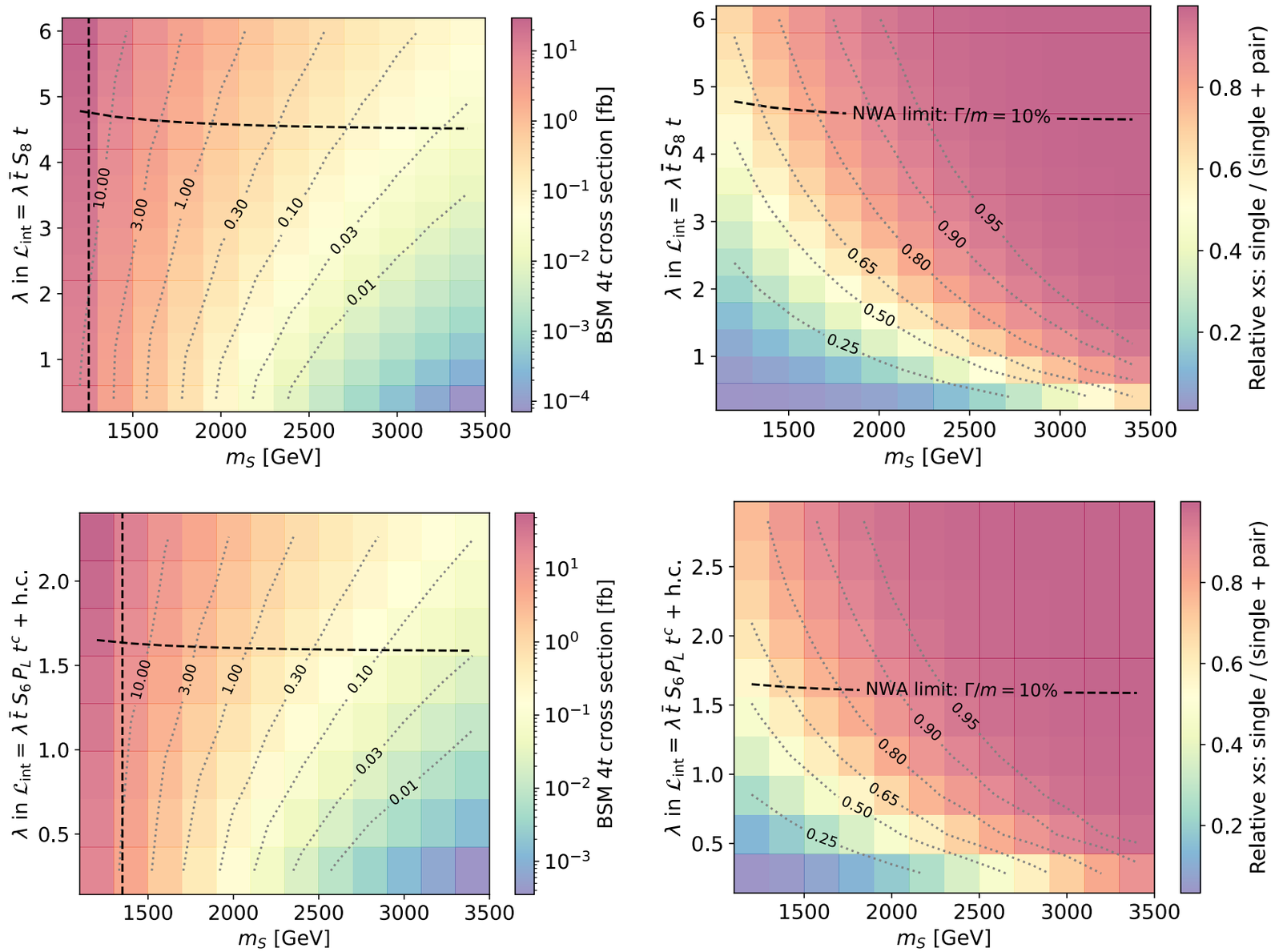


Figure 2. Comparison of single production and pair production of (top) colour octet scalars S_8 and (bottom) colour sextet scalars S_6 with (left) total and (right) relative cross sections calculated at LO. The vertical and horizontal dashed lines indicate the limits from recasts and validity of the narrow width approximation, respectively. Since the single and pair production cannot be cleanly separated, we use $\sigma(pp \to 4t; S_8) - \sigma(pp \to S_8 S_8)$ as a proxy for single production, where "; S_8" indicates that at least one S_8 has to occur (analogous for S_6). This is only a good approximation if interference effects are small.

Machine Learning applied to BSM searches: 4-top events from BSM colored resonances

Event simulation and pre-selection:

- Simulation chain: Feynrules → Madgraph5 → Pythia8 → Delphes3.4.1 →Fastjet3.3.1
- #events
  Signal: 6m events per benchmark mass (1.2 TeV - 2.5 TeV in 100 GeV steps)
  Background: 4t (4.2m), tth (70m), ttV (150m), ttVV (4.3m), VVV (48m)
- basic selection cuts:
  - exactly 2 same-sign leptons
  - at least 3 b-tagged jets
  - at least 3 (more) jets
  - mild missing p_T cut (20 GeV)
  - mild S_T cut (400 GeV)
  - standard lepton isolation and rapidity criteria (ATLAS config)

Machine Learning applied to BSM searches: 4-top events from BSM colored resonances

Data & data-pre-processing

Kinematic data:

We demand 2 leptons, 3 jets, 3 b-jets and construct from them 51 kinematic observables

$$\mathcal{K} = \bigcup_{i \neq j} M_{ij} \cup \bigcup_{i \neq j} \Delta R_{ij} \cup \bigcup_{i} p_{Ti} \cup \{\not{E}_T, S_T\}$$

Jet images:

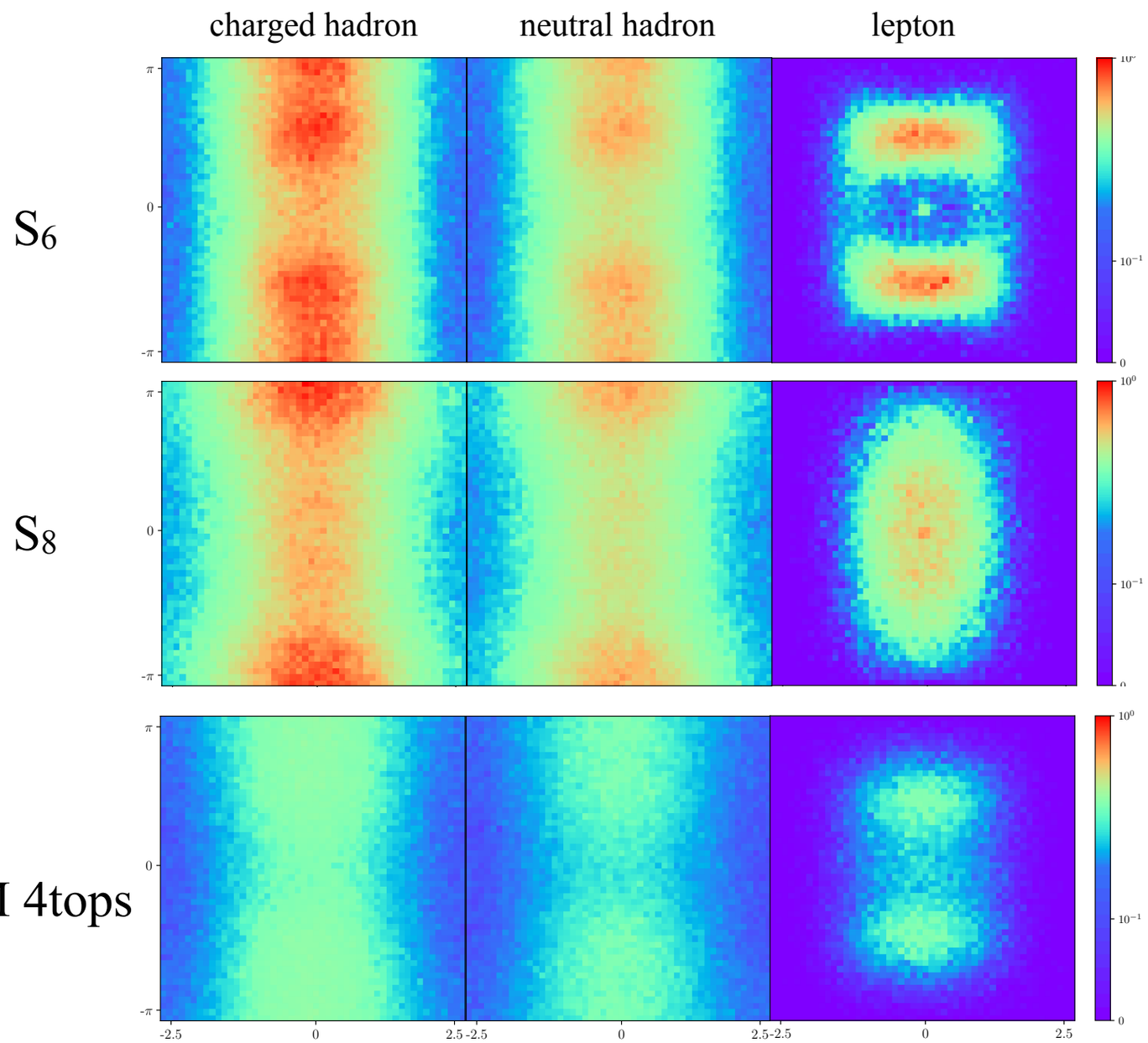
For each event, we determine an angular maps in the following way:

1. Set the center of the (η,ϕ) plane as the midpoint between the two same-sign leptons.

2. Determine the (η,ϕ) map of the p_T of (a) charged "jets", ((b) neutral "jets",) (c) di-leptons by binning objects of the respective class in a 50x50 grid and and summing the p_T in each bin to obtain the pixel intensity

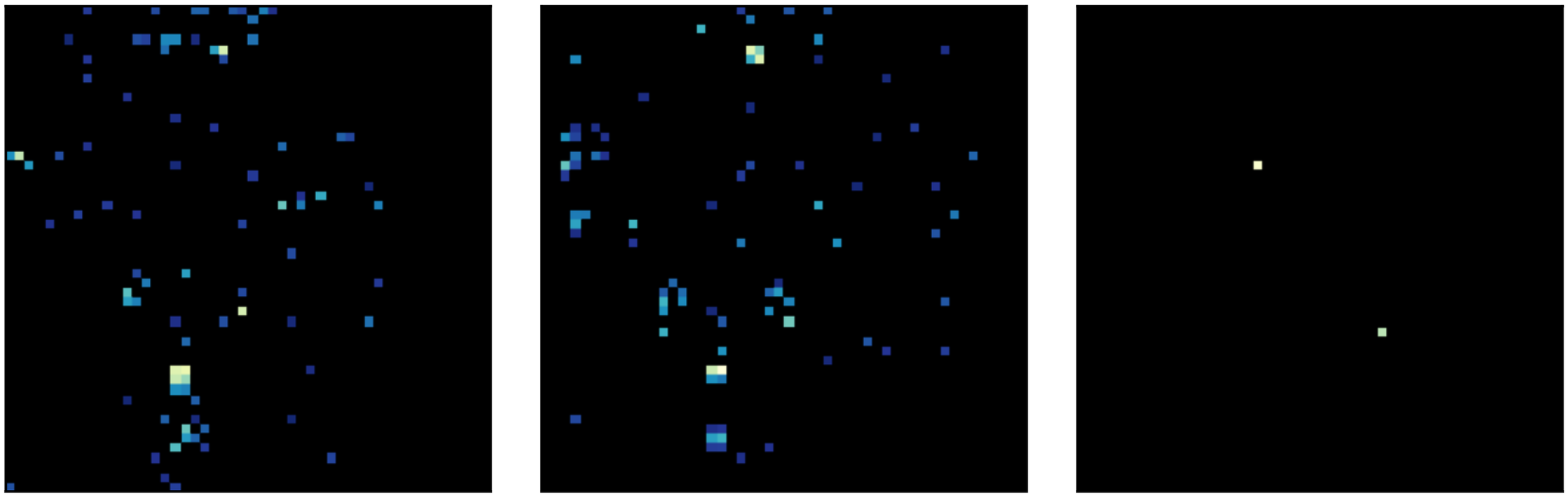
→ $V_{\text{image}}^{(C,\ell)} = (2 \times 50 \times 50)$ or $V_{\text{image}}^{(C,N,\ell)} = (3 \times 50 \times 50)$

Machine Learning applied to BSM searches: 4-top events from BSM colored resonances



overlaid jet images (main background and signal classes)

Machine Learning applied to BSM searches: 4-top events from BSM colored resonances



single jet images are sparse

Machine Learning applied to BSM searches: 4-top events from BSM colored resonances

Network candidate 1: Convolutional Neural Network (CNN) combined with a Fully Connected Deep Neural Network (DNN)

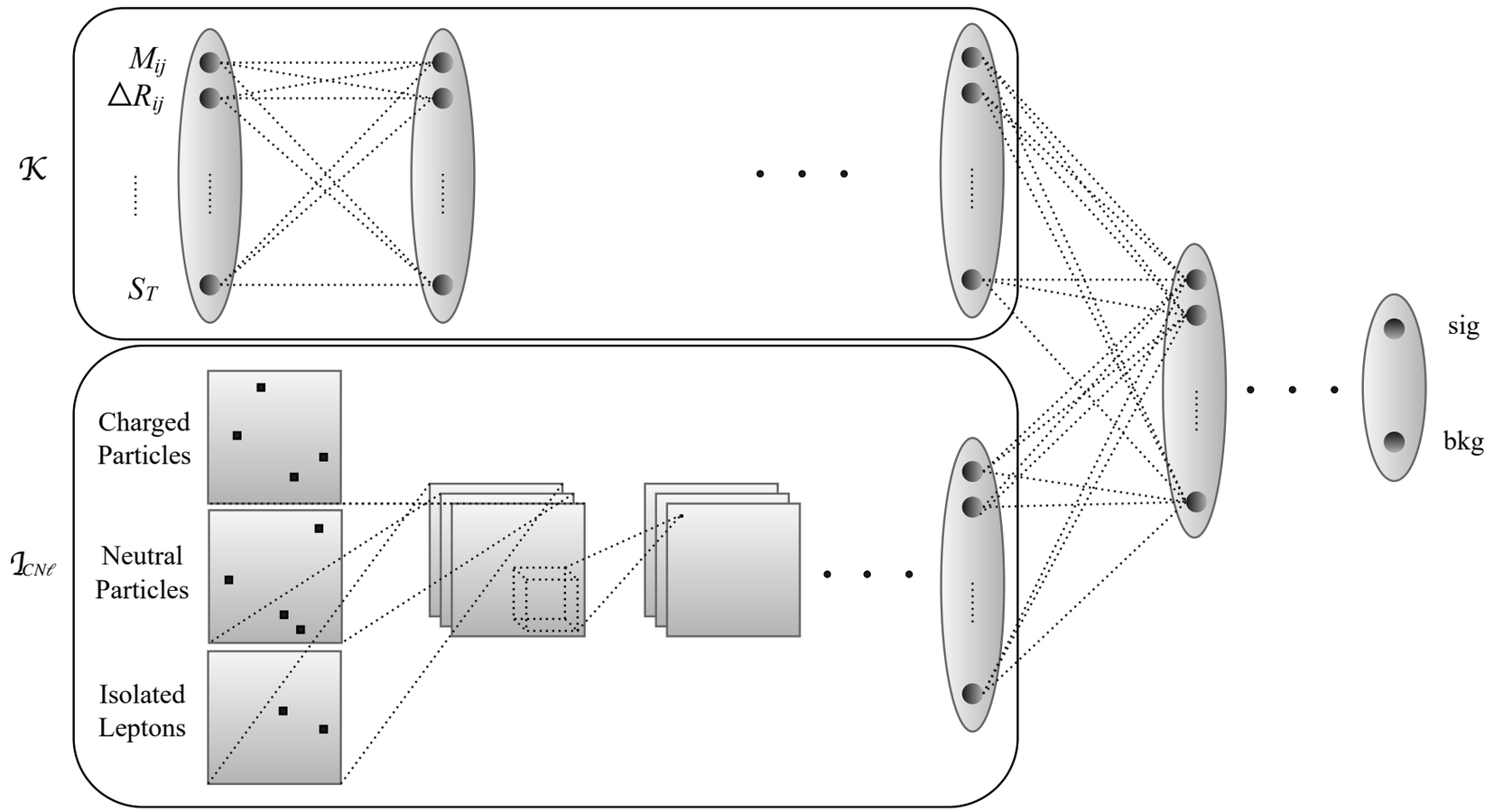


Figure 5. A schematic architecture of the neural networks used in this paper. The separate DNN chain in the upper panel is used only when the kinematic variables are included.

Machine Learning applied to BSM searches: 4-top events from BSM colored resonances

Network candidate 2: Shifting window (Swin) Transformer

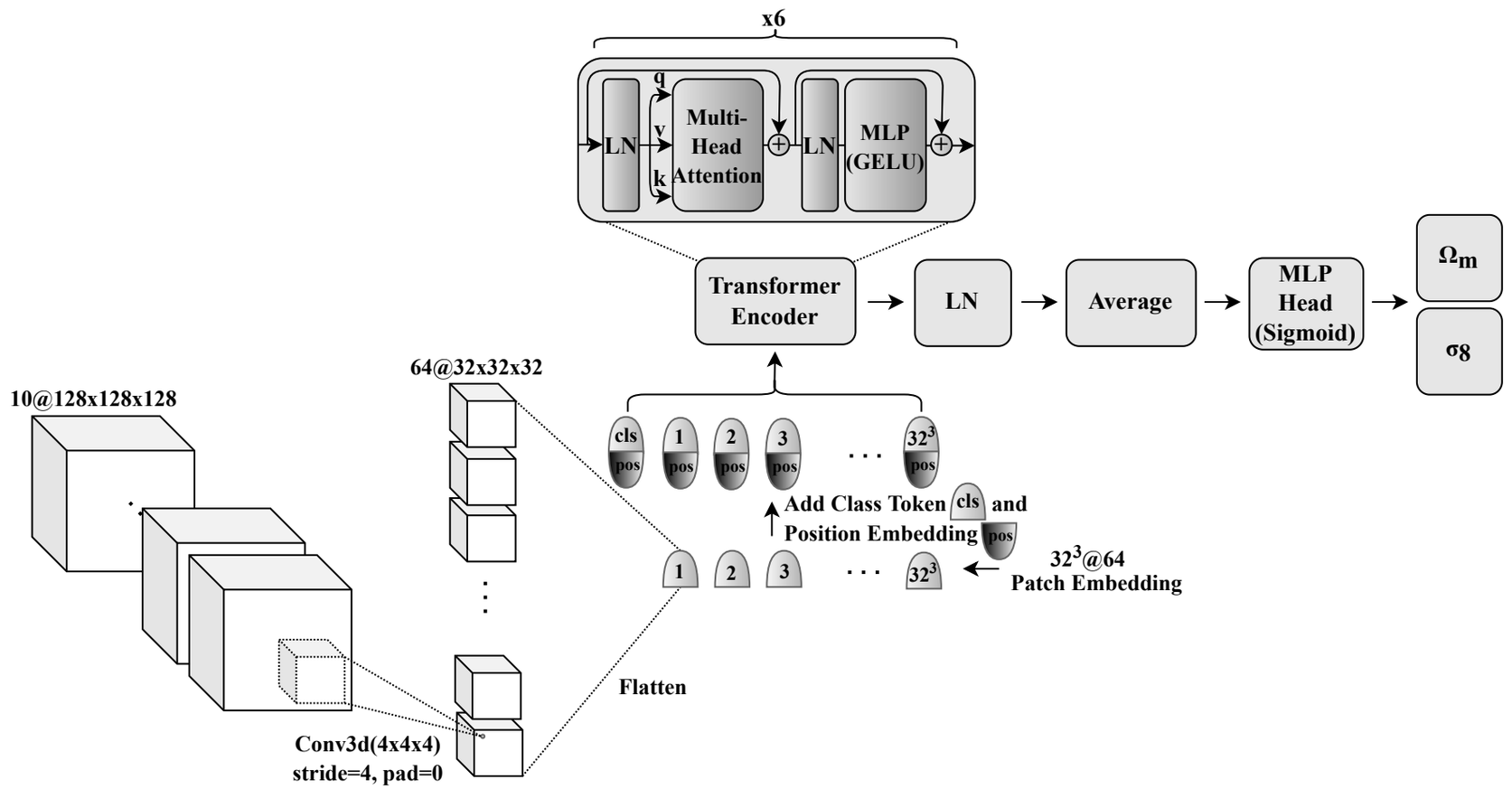
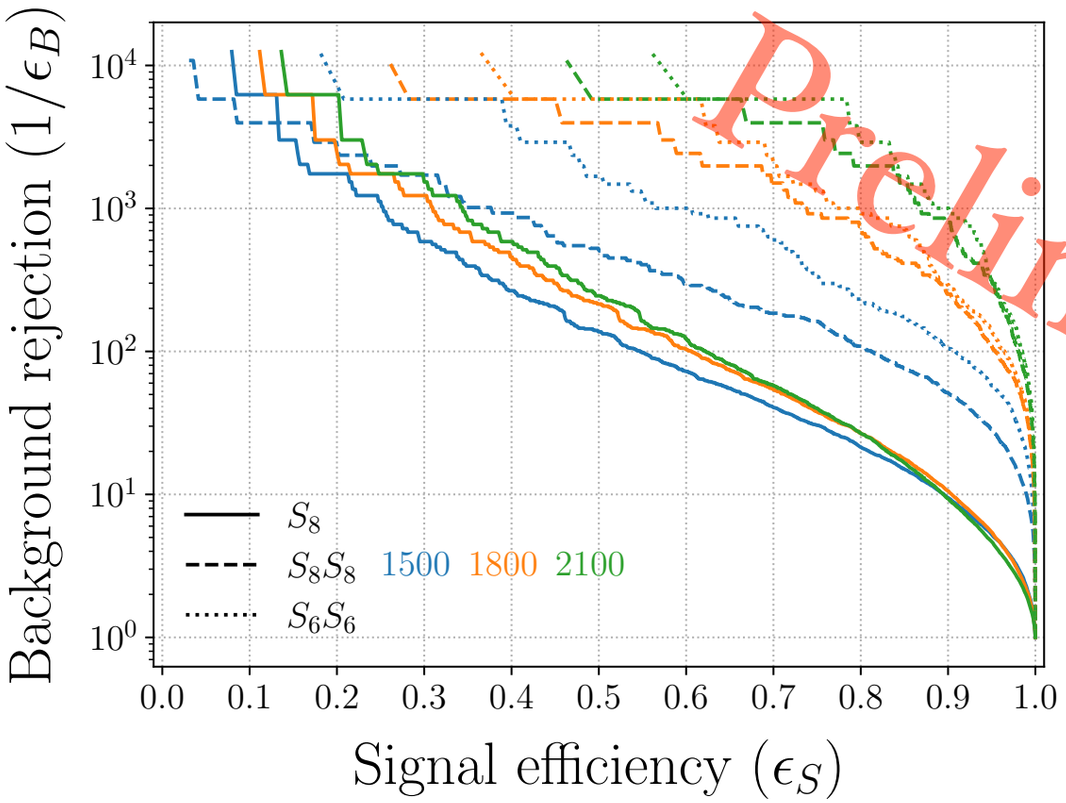
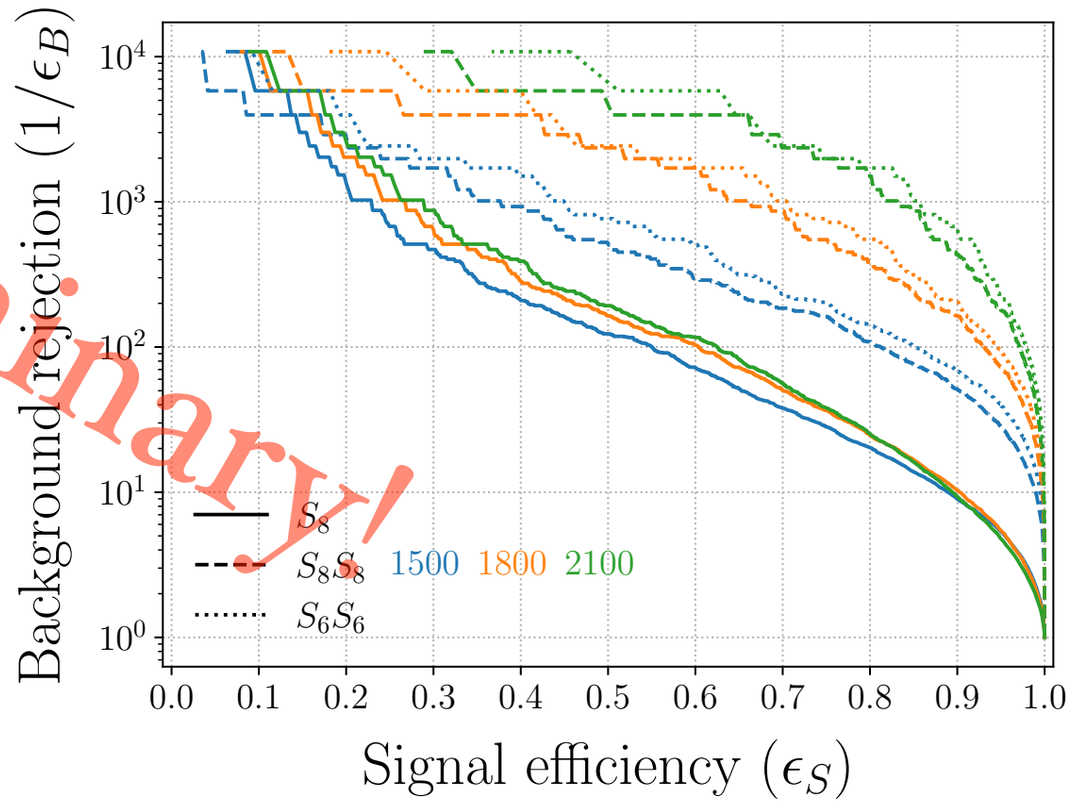


Figure 15. A schematic architecture of Swin Transformer used in this paper.

Task 1: Distinguishing signal from background



(a) CNN

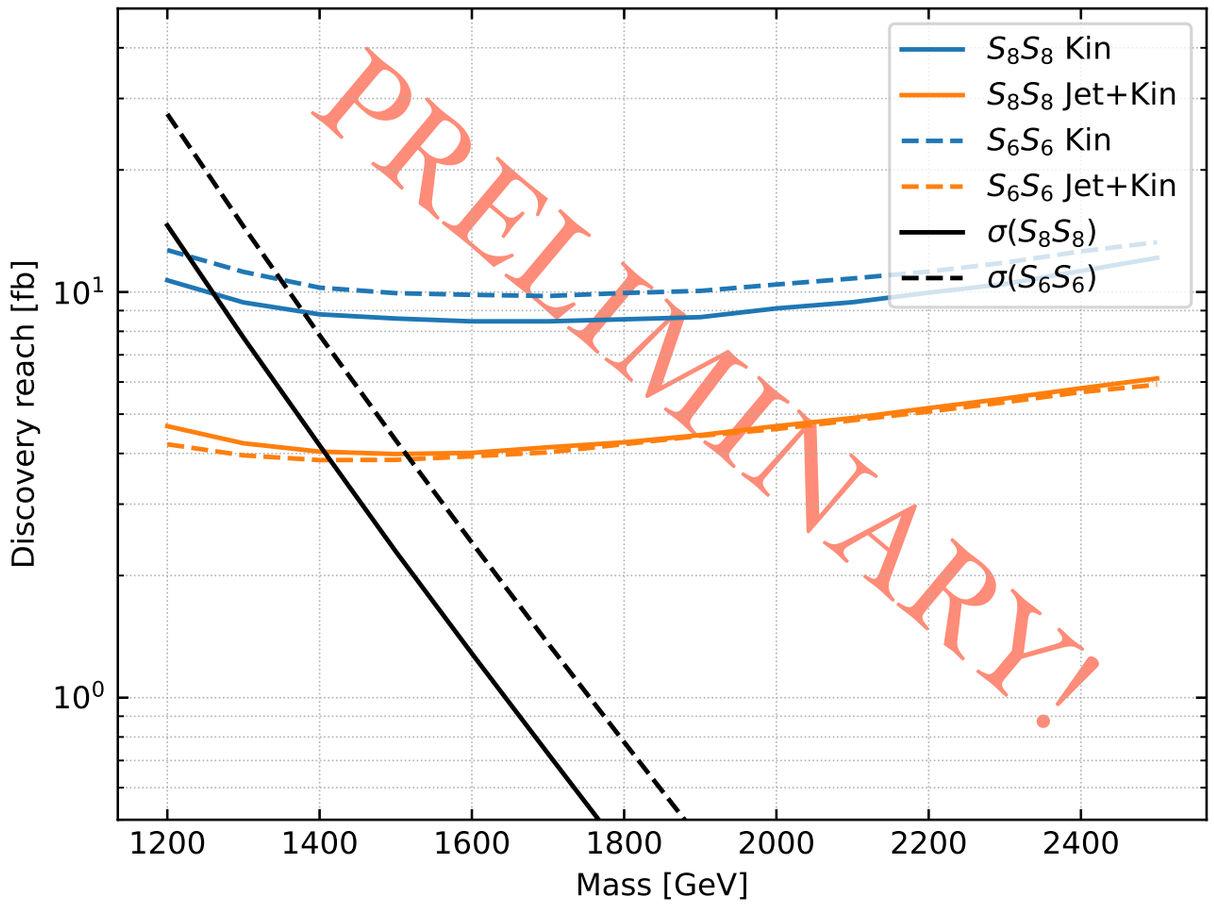


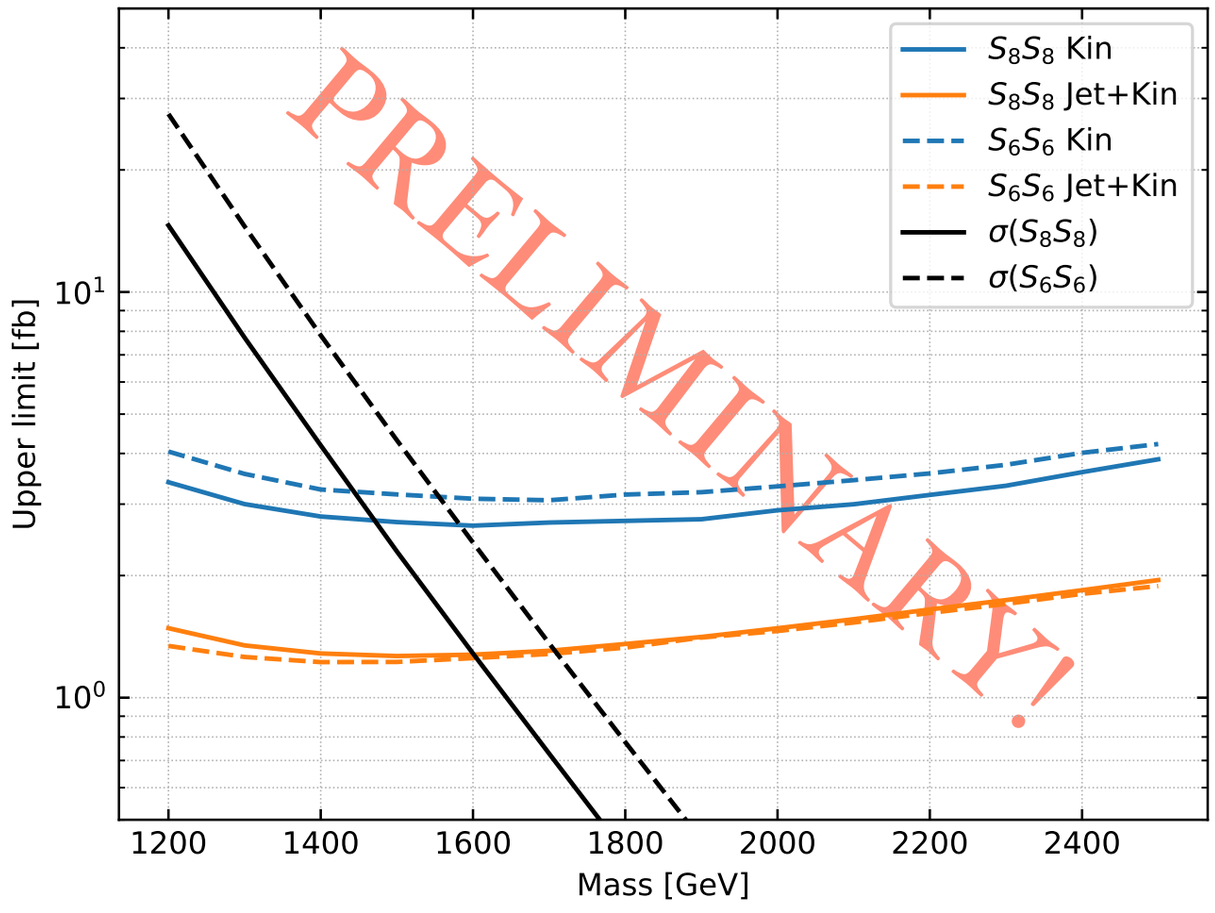
(b) Swin Transformer

Preliminary!

Task 1: Distinguishing signal from background

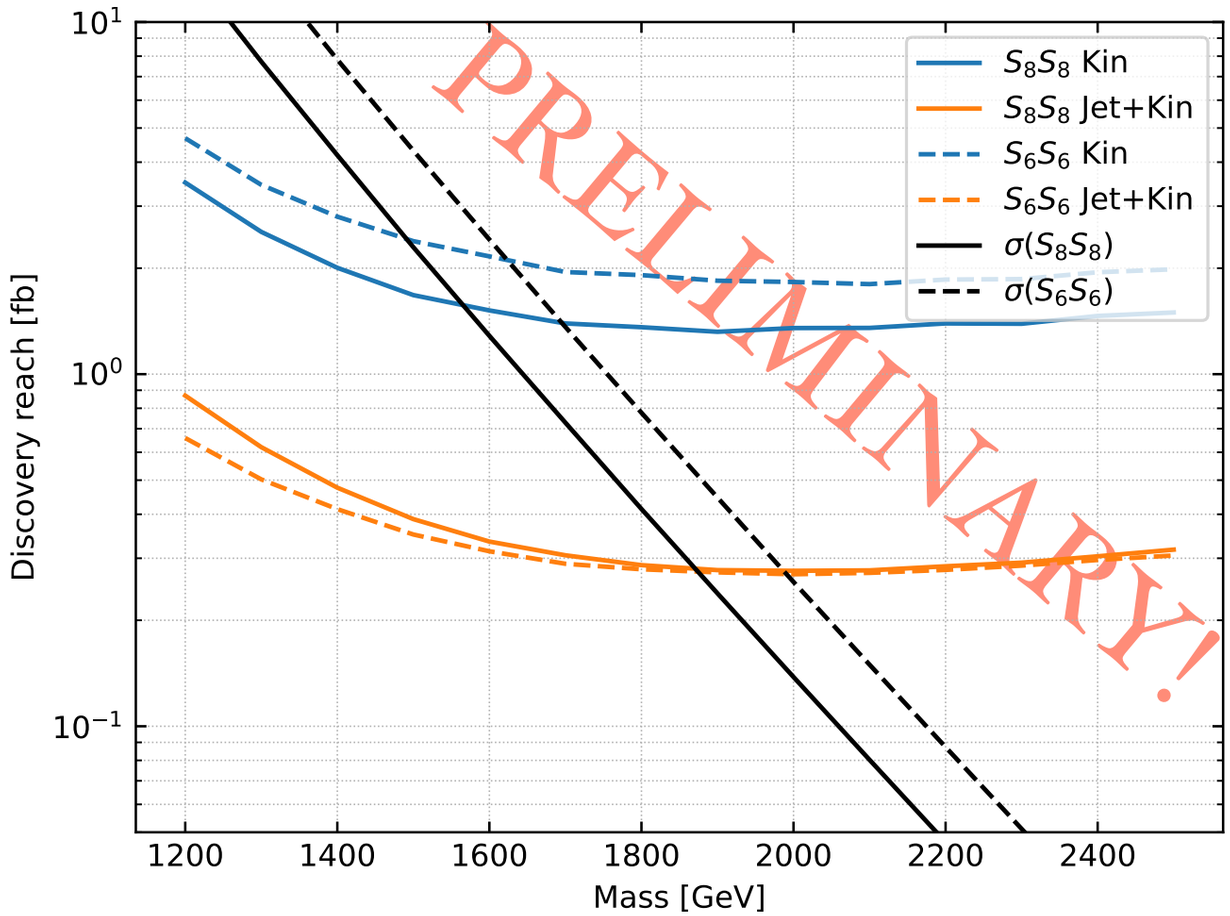
predicted discovery and exclusion reach at the LHC (now; 139 fb^{-1})

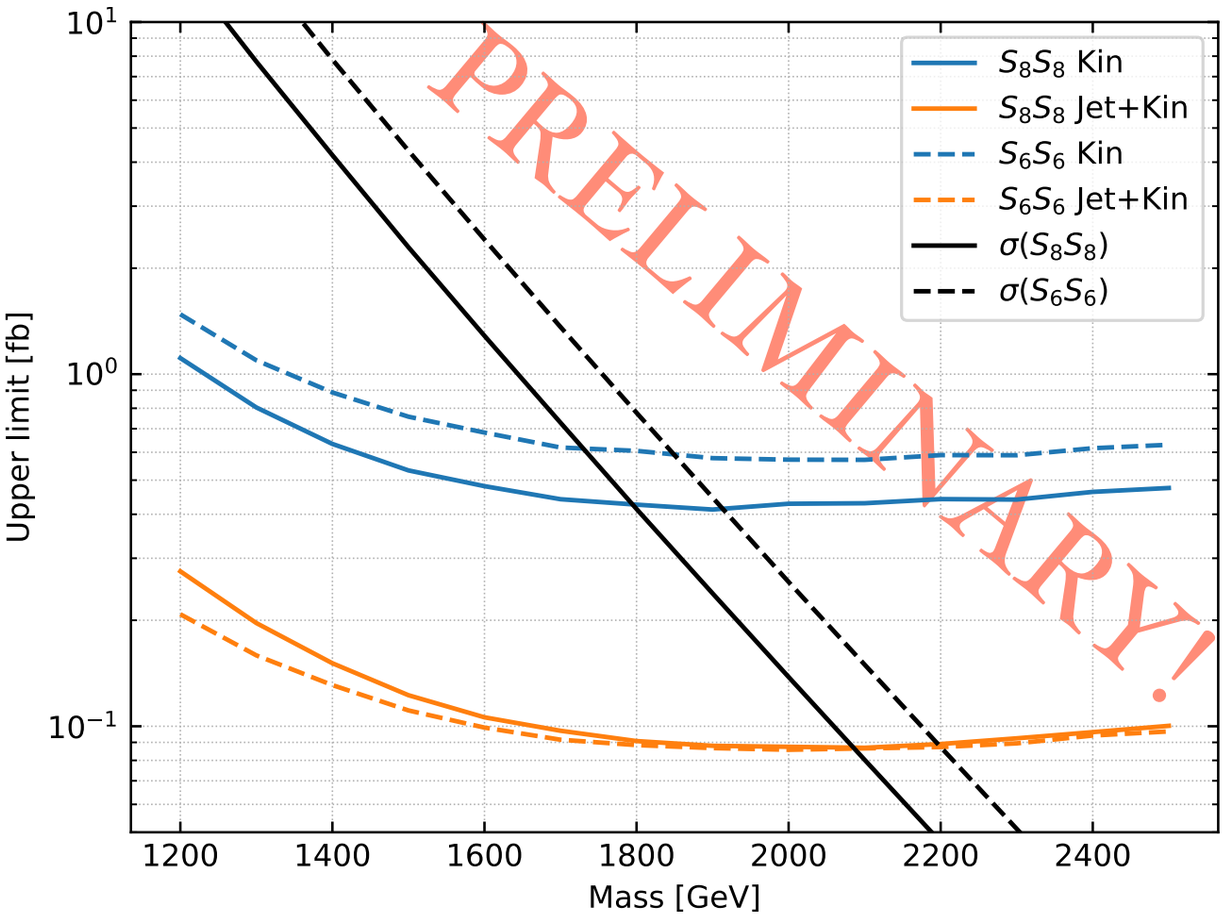




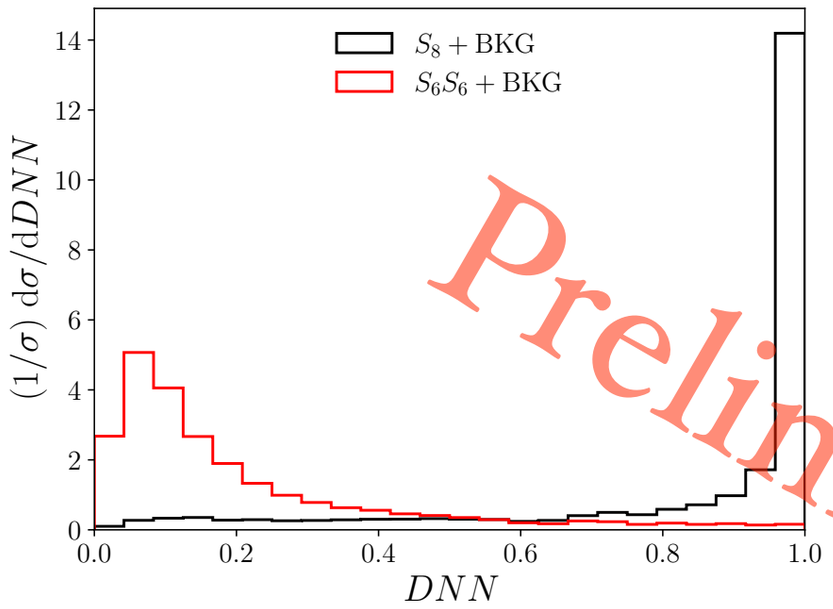
Task 1: Distinguishing signal from background

predicted discovery and exclusion reach at the LHC HL (3000 fb^{-1})

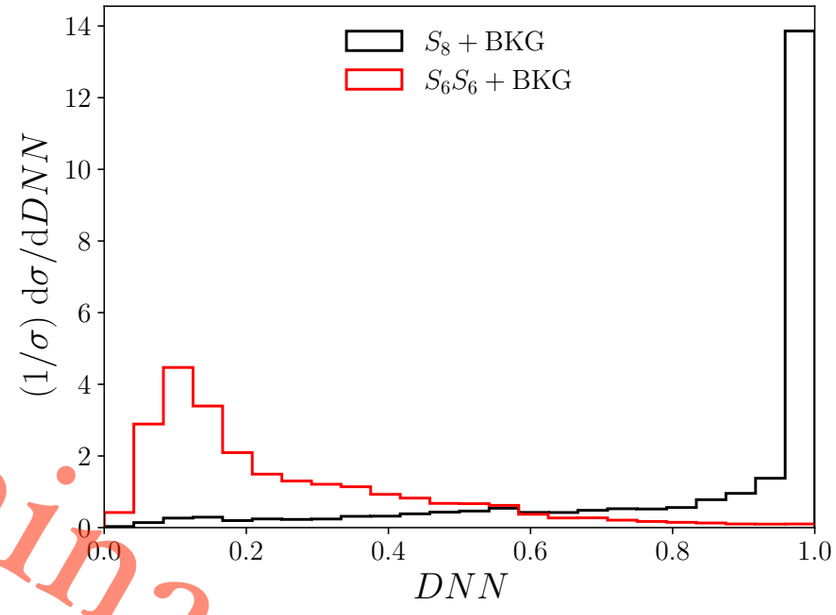




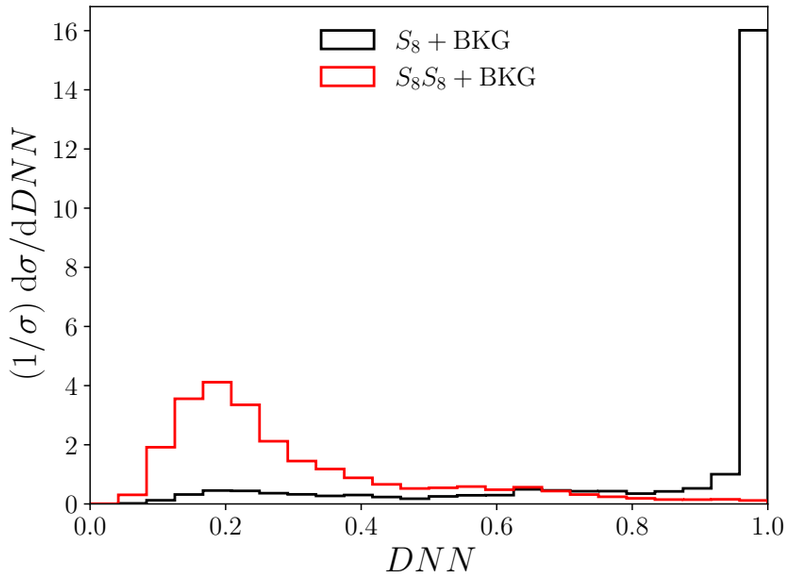
Task 2: Distinguishing sextet pair production, octet pair production, and single production



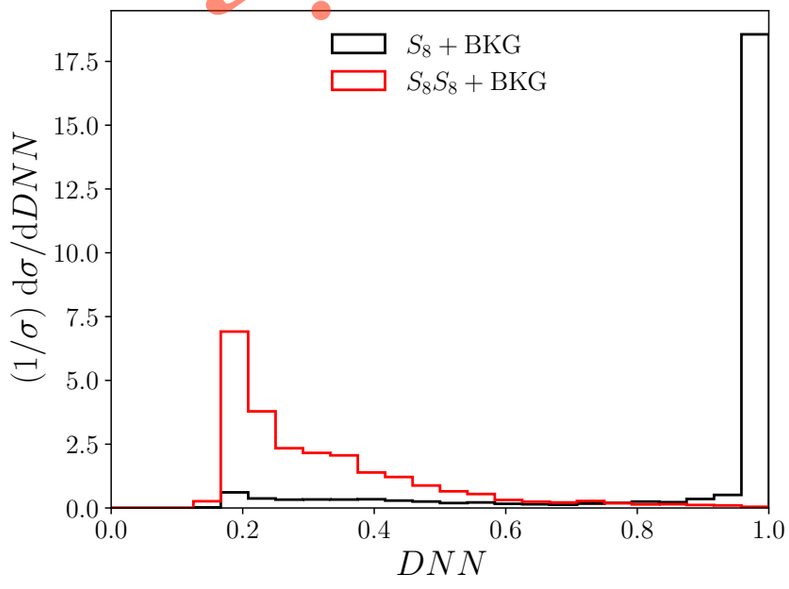
(a) S_6S_6 vs S_8, Signal discrimination, CNN



(b) S_6S_6 vs S_8, Signal discrimination, Swin Transformer



(a) S_8S_8 vs S_8, Signal discrimination, CNN

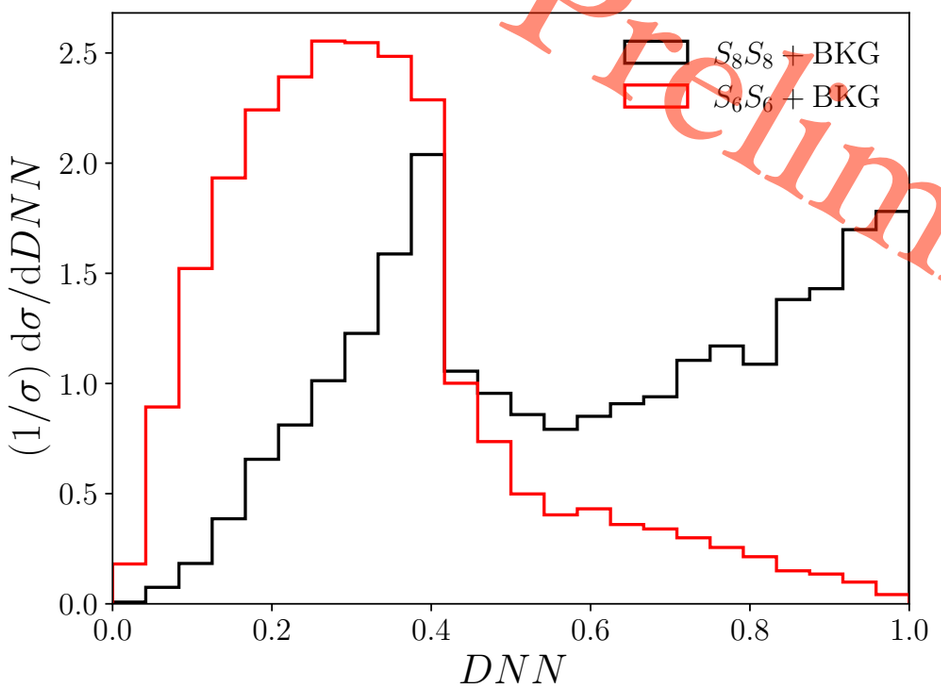


(b) S_8S_8 vs S_8, Signal discrimination, Swin Transformer

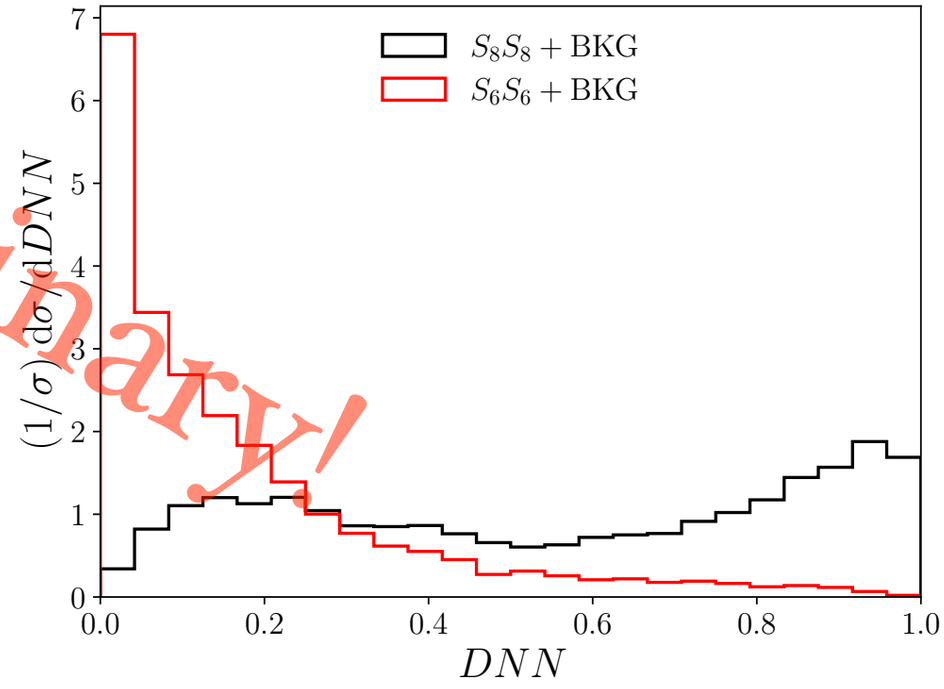
Preliminary!

Task 2: Distinguishing sextet pair production, octet pair production, and single production

Preliminary!



(a) S_6S_6 vs S_8S_8, Signal discrimination, CNN



(b) S_6S_6 vs S_8S_8, Signal discrimination, Swin Transformer

Summary & Outlook

- Many BSM models predict BSM colored states (in various color representations) which can decay into top quarks.
- Current LHC searches for 4-top events constrain color octets (sextets) to be heavier than 1.2 TeV (1.3 TeV).
- The studied combination of a DNN for kinematic information and a convolutional neural network for jet images provide excellent performance on 4-top final states with 2 same-sign leptons and many hadrons in signal detection, and model discrimination.
- Inclusion of jet images yields substantial improvement in performance.
- The studied Swin Transformer provides comparable performance.
- Analysis of NN uncertainties is under way.

Backup

Machine Learning applied to BSM searches: 4-top events from BSM colored resonances

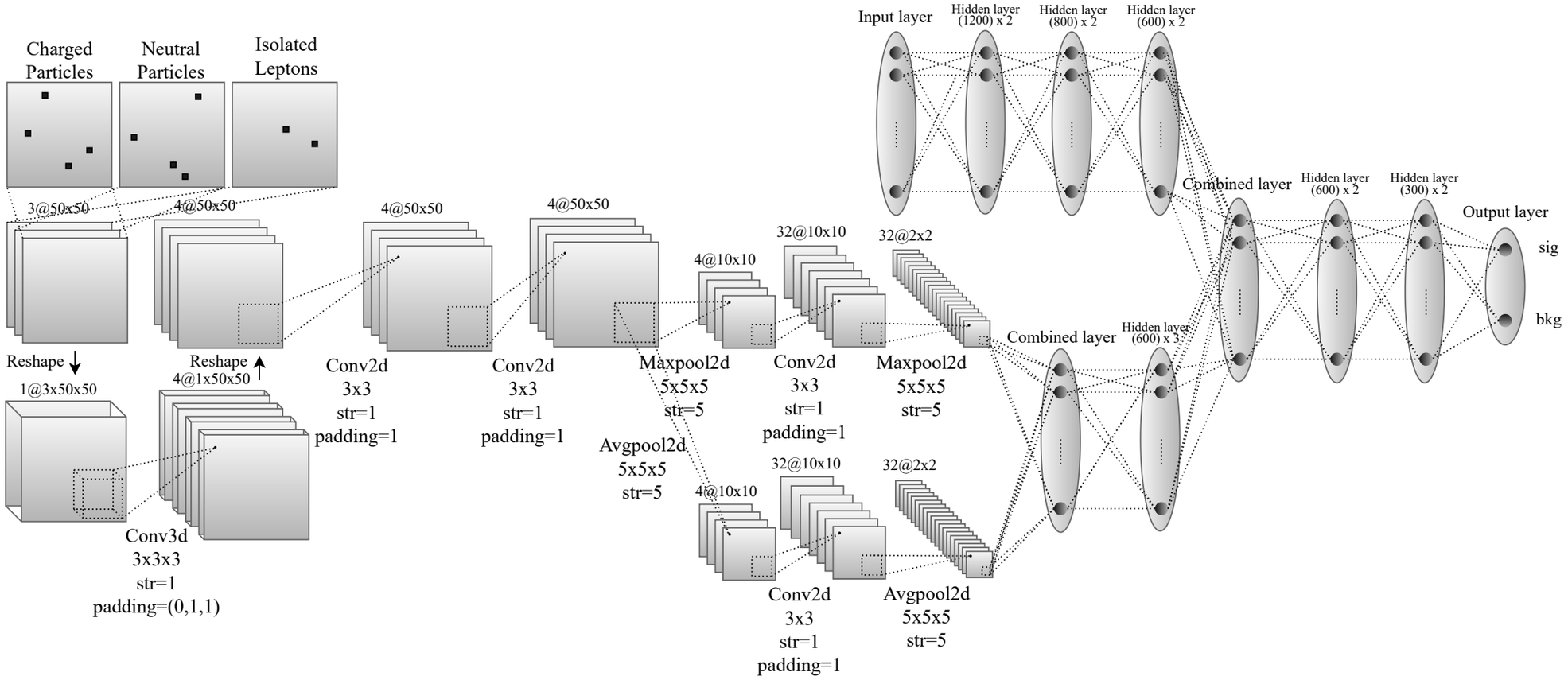


Figure 9. A schematic CNN architecture used in this article. The separate FC chain in the right-upper corner is used only when kinematic variables are included.